MethodsX 12 (2024) 102778

Contents lists available at ScienceDirect

MethodsX

journal homepage: www.elsevier.com/locate/methodsx

Enhanced mangrove index: A spectral index for discrimination understorey, nypa, and mangrove trees

Bayu Prayudha[a,d], Yaya I. Ulumuddin[a], Vincentius Siregar[b,*], Suyarso[a], Syamsul B. Agus[b], Lilik B. Prasetyo[c], Suyadi[e], Praditya Avianto[a], Muhammad R. Ramadhani[a]

[a] *Research Center for Oceanography, National Research and Inovation Agency (BRIN), Jl. Pasir Putih I, Ancol Timur 14430 Jakarta Indonesia*
[b] *Department of Marine Science and Technology, Faculty of Fisheries and Marine Sciences, IPB University, Jl. Raya Dramaga, Kampus IPB, Dramaga Bogor 16680 Jawa Barat, Indonesia*
[c] *Department of Forest Resources Conservation and Ecotourism, Faculty of Forestry and Environment, IPB University, Jl. Raya Dramaga, Kampus IPB, Dramaga Bogor 16680, Jawa Barat, Indonesia*
[d] *Postgraduate School, Department of Marine Science and Technology, Faculty of Fisheries and Marine Sciences, IPB University, Jl. Raya Dramaga, Kampus IPB, Dramaga Bogor 16680 Jawa Barat, Indonesia*
[e] *Research Center for Ecology and Ethnobiology, National Research and Inovation Agency (BRIN), Jl. Raya Jakarta-Bogor No.Km.46, Cibinong, Bogor 16911 Jawa Barat, Indonesia*

ARTICLE INFO

Method name:
Enhanced Mangrove Index (EMI)

Keywords:
EMI
Classification
Mangrove mapping
Invasion
Segara anakan

ABSTRACT

Unsupervised classification using vegetation indices has been extensively employed to map mangrove forests using medium-resolution satellite images. However, its capability is restricted to determining the extent of mangroves only. This study introduces a new spectral index called the enhanced mangrove index (EMI) for accurately mapping different components of mangrove vegetation, including mangrove trees, nypa, and understorey. An immediate effort is required to monitor the invasion of nypa and understorey in the mangrove forest of Segara Anakan Lagoon, located in Central Java, Indonesia. This issue may also be prevalent in other mangrove areas worldwide. The development of EMI involved: 1). the analysis of the reflectance exhibited by different types of mangrove vegetation, and 2). The performance of EMI was evaluated by comparing it with spectral indices such as automated mangrove map and index (AMMI), as well as supervised classification models like random forest (RF). The accuracy assessment indicates that the overall accuracy and Kappa coefficient achieved values of 0.87 and 0.84, respectively, surpassing other spectral indices and supervised classification models. AMMI and RF exhibited high overall accuracy, with values of 0.82 and 0.73, respectively. Additionally, they demonstrated a Kappa coefficient of 0.77 and 0.66, respectively.

Specifications table

Subject area:	Environmental Science
More specific subject area:	Remote Sensing
Name of your method:	Enhanced Mangrove Index (EMI)
Name and reference of original method:	Not applicable
Resource availability:	Not applicable

* Corresponding author.
E-mail address: vincentius@apps.ipb.ac.id (V. Siregar).

https://doi.org/10.1016/j.mex.2024.102778
Received 12 February 2024; Accepted 24 May 2024
Available online 25 May 2024

Method details

Rationale

The overexploitation of mangrove forests is a worldwide issue, resulting in a 4 % reduction in their global area [6]. This decline occurred at an average annual rate of 0.21 % between 1996 and 2016. Additionally, it is stated that Southeast Asia experiences the second highest rate of mangrove depletion (0.29 % annually), primarily due to the expansion of aquaculture, agriculture, and oil palm plantations. Indonesia, possessing 3.2 million hectares of mangrove forest, encounters a comparable circumstance [11,20], with a 20 % reduction in mangroves from 1989 to 2009, equating to an annual loss of approximately 2 %.

Segara anakan lagoon (SAL) in Cilacap, Central Java, is an example of Indonesia's mangrove forest that has been degraded due to various factors including sedimentation, logging, conversion of land for agriculture and aquaculture, and pollution. These drivers have been documented in studies by Yuwono et al. [42], Ardli and Wolff [2], Jenerjahn and Yuwono [21], Syakti et al. [35], and Lukas [26]. The lagoon has experienced significant sedimentation since the 17th century due to erosion in its surrounding area. This has led to a reduction in the lagoon's size, leaving only one-fourth of its original water area compared to its condition in 1857 [26]. The water salinity is progressively diminishing and has the potential to reach a value of zero, especially in the western region during the rainy season [17]. The alterations result in the displacement of mangrove communities in SAL, as nypa and understorey communities invade and supplant mangrove trees [30].

Remote sensing has become more prevalent in recent years for the efficient monitoring of mangrove forests, especially in remote and inaccessible regions [24,37]. The study of mangrove mapping has been conducted for approximately six decades utilizing satellite imagery with moderate spatial resolution. However, there persist challenges, as highlighted by Wang et al. [37], for example, the erroneous identification of understorey coverage as dense mangrove forest in Segara Anakan, as noted by Winarso et al. [38,39]. In the case of mangrove monitoring in Segara Anakan, detecting nypa in the mangrove matrix is also difficult, as it is limited to high-resolution or synthetic aperture radar and LiDAR [1], or medium-resolution when combined with unmanned aerial vehicles [28]. Indeed, the identification of understorey and the encroachment of nypa palm in Segara Anakan is crucial for monitoring the decline of mangrove trees in the area.

The objective of this research is to develop a spectral index capable of differentiating between mangrove trees and other types of vegetation cover such as nypa and understorey. Xue et al. [41] define a spectral index as a mathematical expression that integrates pixel values from multiple spectral bands within a multispectral image through the use of various algorithms, with band ratio or feature scaling taking the primary emphasis. Spectral indices are computed to highlight a particular ecological function while also indicating the relative abundance of a particular land cover in an image [7,41]. Spectral indices are a commonly employed unsupervised classification method that is widely utilized and effective for land cover and land use classification. Additionally, they are considered to be a more economically efficient computing approach compared to other forms of pixel-based classification, whether it is unsupervised or supervised classification.

Within the realm of spectral indices, the normalized difference vegetation index (NDVI) is frequently employed to differentiate mangrove coverage. However, caution must be exercised when utilizing this particular spectral index. For instance, Winarso et al. [38] noted that the understorey in Segara Anakan is categorized as dense mangrove forests based on the utilization of NDVI. Therefore, they introduced a spectral index called the Mangrove Index (MI) to differentiate between understorey and mangrove trees. However, this index has not been applied for discerning nypa from the matrix of mangrove trees. Several additional spectral indices have been created to distinguish mangrove pixels from non-mangrove pixels, such as Automatic Mangrove Map and Index (AMMI), Mangrove Vegetation Index (MVI), and Combined Mangrove Recognition Index (CMRI) [4,14,34]. However, these indices have only been used to determine the extent and distribution of mangroves and have not been applied for any other purpose, such as identifying understorey or nypa palm. In our knowledge, only Prayudha et al. [29] employed MVI to differentiate understorey, nypa, and mangrove trees; and they achieved a total accuracy of 78.79 % with the Kappa coefficient of 0.73. Hence, the specific objective of this study is to evaluate and contrast various indices and develop a novel spectral index for the classification of satellite images, specifically focusing on understorey, nypa, and mangrove trees. The findings of this study potentially yield insights into the encroachment of understorey, invasion by nypa palm, or shifts in the vegetation community, primarily within the distinct SAL mangrove forests.

Methodology

Description of study area

Segara Anakan Lagoon (SAL) is located in the middle-west of the south part of Java Island, belong to the Central Java Province (Fig. 1). The only estuarine mangrove on Java Island is found in this area, occupying three-quarters of the lagoon [2,17]. Nusakambangan, an island in the south, separates the lagoon and the Indian Ocean. Two outlets in the West and East of the lagoon serve to provide water circulation in and out of the lagoon and the ocean. Located in the west, the Citanduy River provides a substantial amount of freshwater discharge and sediment, resulting in new islands [15,17]. The freshwater from the rivers east of the lagoon does not affect the lagoon much, as the discharge is low. The seawater discharge contributes more to the water circulation in the east part of the lagoon [17,42]. Hence, the mangrove trees community can develop well due to its high salinity environment [27]. The different salinity profiles between the eastern, central, and western parts have contributed to the variation of mangrove communities [17], see Fig. 1. Understorey and nypa dominate land cover in the central and western parts of SAL, while the mangrove trees are relatively dense in the eastern part. Understorey and nypa can adapt to moderate and low soil salinity. Further, the log-

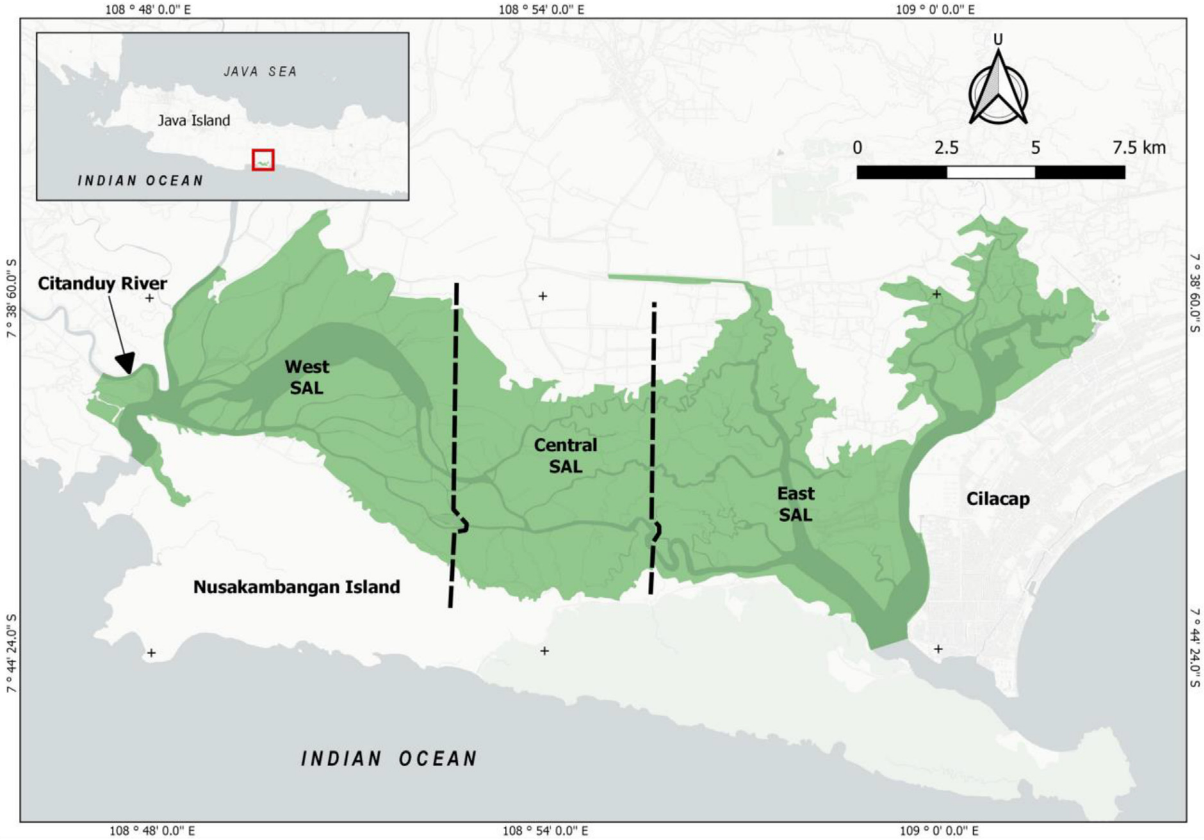

Fig. 1. Map of the study area, Cilacap, Central Java, Indonesia.

ging activity in the central part has exaggerated the encroachment of the understorey, which rapidly invaded the abandoned gaps [3,16,27].

Classification system and sample points

The classification of mangrove vegetation covers in this study is based on the system developed by Saenger [32], as well as the definitions provided by Duke [8] and FAO [9]. These classifications categorize mangrove communities into three groups: trees, palm, and shrub/understorey (see Table 1). This study employed nypa instead of palm, as it was the sole palm species present in the study area. The mixed class refers to pixels in this image that cannot be classified as mangrove trees, nypa, or understorey. A total of 10,140 sample points were gathered from the study site, Segara Anakan, which encompassed various types of vegetation covers, 997 points from the class of mangrove trees, 586 points from nypa, 1145 points from the understorey, and also 7412 points from terrestrial vegetation. The vegetation sample points were determined by analyzing drone photographs and utilizing the high-resolution images from Google Earth. The provided sample points were utilized to illustrate the distinct reflectance patterns exhibited by each vegetation class. Subsequently, a novel spectral index was formulated based on these patterns.

Using a total of 150 sample points from a drone survey, the ability of the new spectral index to discriminate vegetation classes was compared to the other nine spectral indices (Table 2). Statistical tests (ANOVA and Tukey's) were used to assess the discriminatory ability of spectral indices in distinguishing between mangrove trees, nypa, and understorey.

Data used and pre-processing

The main sources of data utilized in this research were Landsat 8 OLI images, although not exclusively from this Landsat series. The Landsat series was chosen because it has long-term archives dating back to 1972 [25,36,40]. It is useful for mangrove forest monitoring, which typically requires historical data to track changes over time [5]. This study specifically used multiple images from the Landsat 8 OLI Surface Reflectance (SR) product archive from 2017 to 2019 to create a single cloud-free image. The process involved masking the cloud object using the Landsat dataset's quality band and combining the images based on their median value [33]. All data was acquired and processed using Google Earth Engine's (GEE) cloud computing service.

Table 1
The type of mangrove vegetation cover, drone view (top and oblique).

Classes	Nadir View	Off-nadir View
Mangrove Trees		
understorey		
nypa		
Mixed		

Table 2
The various type of spectral indices used in this study.

No	Spectral Indices	Formula	Source	Notes
1	NDVI (Normalized Difference Vegetation Index)	(NIR - RED) / (NIR + RED)	Rouse et al. [31]	
2	SAVI (Soil-Adjusted Vegetation Index)	(NIR - RED) / (NIR + RED + L)	Huete [18]	L = a constant to eliminate the influence of soil background (0 - 1); L = 0.5 (medium canopy coverage); L = 0.75 (dense canopy coverage)
3	ARVI2 (Adjusted Resistant Vegetation Index 2)	−0.18 + 1.17 * ((NIR - RED) / (NIR + RED))	Gitelson et al. [13]; Kaufman and Tanre [23]	
4	EVI (Enhanced Vegetation Index)	G * ((NIR - RED) / (NIR + c1 * RED - c2 * BLUE + L)	Huete et al. [19]	The constant value refers to Lagomasino et al., 2014 which was adopted from [18] and Huete et al. 1994, as G = 2,5; c1 = 6; c2 = 7,5; L = 1
5	NDWI (Normalized Difference Water Index)	(NIR - SWIR) / (NIR + SWIR)	Gao [12]	SWIR refers to Band 5 of Landsat TM/ETM+, Band 6 of Landsat OLI, and Band 11 of Sentinel-2
6	MI (Mangrove Index)	((NIR − SWIR) / (NIR × SWIR)) × 10,000	Winarso et al. [38]	SWIR refers to Band 6 of Landsat OLI and Band 11 of Sentinel-2
7	CMRI (Combined Mangrove Recognition Index)	NDVI - NDWI	Gupta et al. [14]	
8	MVI (Mangrove Vegetation Index)	(NIR - GREEN)/(SWIR - GREEN)	Baloloy et al. [4]	SWIR refers to Band 6 of Landsat OLI and Band 11 of Sentinel-2
9	AMMI (Automatic Mangrove Map and Index)	(NIR - RED) / (RED + SWIR) * (NIR - SWIR) / (SWIR - 0.65 * RED)	Suyarso [34]	SWIR refers to Band 6 of Landsat OLI and Band 11 of Sentinel-2
10	EMI (Enhanced Mangrove Index)	(NIR - SWIR) / (GREEN + NIR)	This Study	SWIR refers to Band 6 of Landsat OLI and Band 11 of Sentinel-2

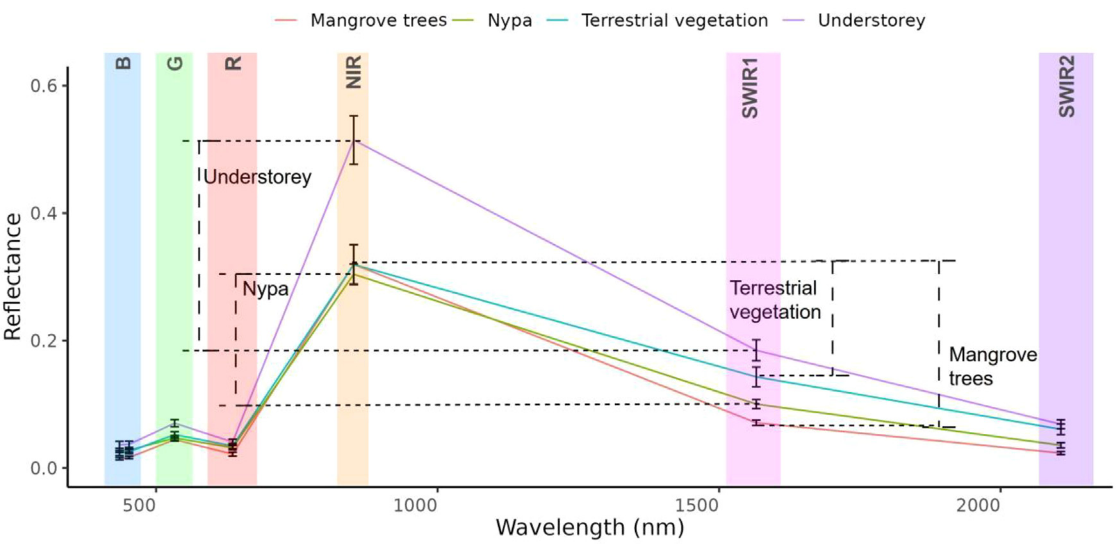

Fig. 2. The spectral reflectance of terrestrial and mangrove vegetation types (trees, nypa, and understorey).

Development enhanced mangrove index

The enhanced mangrove index (EMI) was created by analyzing the spectral reflectance signature of the vegetation classes (Fig. 2), which was generated from Landsat OLI data collected at the sample points. The figure shows that in the NIR (near infra-red) region (700 - 1000 nm), mangrove trees cannot be distinguished from terrestrial vegetation, whereas nypa and understorey have specific reflectance against both mangrove trees and terrestrial vegetation. A similar pattern can also be seen in the green region (± 500 nm). Different patterns were found in the blue (± 400 nm), red (± 600 nm), and SWIR (short wave infra-red) region (1500 - 1800 nm). All vegetation covers absorb light in blue (± 400 nm) and red (± 600 nm) wavelengths. The reflectance of vegetation covers can only be clearly distinguished in the SWIR1 region. As a result, the differences in pattern between SWIR1 and NIR can be used to distinguish between vegetation types of mangrove and terrestrial vegetation. Furthermore, to highlight the differences, the green spectrum can be combined with the NIR because they both have a similar pattern. Huete (2004) noted that green and NIR had similar specific interactions with green leaves and hence both spectra are useful for determining vegetation health. However, the magnitudes of these two spectra differ because the green spectrum continues to absorb significantly in the leaf. Based on these findings, EMI was created to help identify detailed features in mangrove habitats. The formula for the new index is as follows:

$$\left(\mathrm{NIR} - \mathrm{SWIR}_{1500-1800}\right) / (\mathrm{NIR} + \mathrm{GREEN})$$

where $\mathrm{SWIR}_{1500-1800}$ is the SWIR spectrum in the region between 1500 and 1800 nm, and this spectrum region equal to Band 6 of Landsat 8 OLI or Band 5 of Landsat 5–7.

The distinct differentiation between the vegetation types of mangrove and terrestrial vegetation in the SWIR region may be attributed to the specific properties of this spectrum, which exhibits high absorption in water content. The presence of water within the vegetation and soil is a significant factor in determining the composition of remotely sensed imagery [24]. The NIR and SWIR region is valuable for identifying mangrove species because of their fundamental biophysical and chemical characteristics [22,24]. To be more precise, the SWIR region can offer insights into the absorption of radiation by water, cellulose, and lignin [24,36]. Gao [12] demonstrated that the SWIR region is effective for emphasizing the water content within the vegetation canopy. The study confirmed the benefits of utilizing the SWIR region for obtaining data pertaining to the identification of mangroves.

Accuracy assessment

For accuracy assessment, 71 sample points were gathered using field observations and high-resolution images from the ESRI map service. These sample points were separated based on the associated vegetation type, i.e., mangrove trees, nypa, and understorey. The assessment was performed on mangrove classification maps generated from Landsat 8 OLI using the best-selected spectral indices and supervised classification models, such as decision tree models random forest (RF) and classification and regression trees (CART), distance-based models minimum distance (MD), and support vector machine (SVM) [10].

The accuracy assessment utilized a combination of overall, user, and producer accuracy values extracted from the confusion matrix, along with the Kappa coefficient, to evaluate and assess the performance of the models. In order to offer a more comprehensive elucidation, it is imperative to interpret all values in their entirety. The producer accuracy represents the proportion of predicted pixels belonging to a particular class that accurately match the corresponding actual pixels. User accuracy, on the other hand, measures the proportion of correctly predicted pixels in a specific class compared to the total number of predicted pixels. For instance, in a particular scenario, the combined accuracy and the Kappa coefficient serve as indicators of confidence. Conversely, certain classes exhibit low accuracy, while the remaining classes demonstrate high accuracy. Only the producer and user accuracy values can provide this data.

Evaluation on the spectral indices

Selection of spectral indices

The ability of spectral indices to distinguish between objects or land covers is first demonstrated by comparing the histograms of each spectral index (Fig. 3). The number of peaks on the histogram represents variability data, which is most likely associated with different objects. The inter-quartile statistics show that EMI (the new index) and NDWI have the highest peaks, 14 and 13, respectively (Fig. 3). It indicates that those two indices outperform other indices in terms of pixel value sorting. MVI had the least variability, with only three peaks, and thus appeared to perform poorly for mangrove classification, despite performing well for distinguishing mangroves from other objects [4].

Further evaluation of the spectral indices utilizing ANOVA and Tukey's test indicates that mangrove vegetation types can be distinguished by EMI, AMMI, and NDWI (Fig. 4). As illustrated by the box plot graph constructed from the 150 sampling points, as mentioned before, the indices were utilized to differentiate between various types of mangrove vegetation. The distinguished letters serve to indicate the significant distinction among the classes ($p < 0.05$). The formulas for these indices utilize the SWIR spectrum in comparable fashions (Table 2). However, it should be noted that MVI, MI, and CMRI, which also rely on the SWIR spectrum, exhibit suboptimal performance in differentiating mangrove vegetation types. This is due to their inability to demonstrate a substantial distinction between mixed and nypa classes. On the contrary, spectral indices that do not incorporate SWIR fail to denote the capacity to differentiate among every type of mangrove vegetation. The results indicate that the SWIR spectrum may, to a certain degree, enhance the capability of spectral indices to differentiate mangrove trees, nypa, and understorey. As a result, NDWI, EMI, and AMMI are chosen for additional validation.

Threshold value

The spectral indices mentioned above can be easily used for image classification once the range or threshold value has been determined. Each class of mangrove vegetation type has its own exclusive spectral index threshold value; for one class to be greater than another in terms of spectral index value, that class must be distinguished. To illustrate, mangrove trees have the highest EMI value, followed by nypa, mixed class, and understorey (Fig. 4). The difficulty arises when determining the minimum threshold of mangrove trees and the maximum threshold of nypa, which must be extremely similar, as shown in the figure. To determine the minimum threshold value for mangrove trees or the maximum threshold value for nypa, use the following equation and illustration:

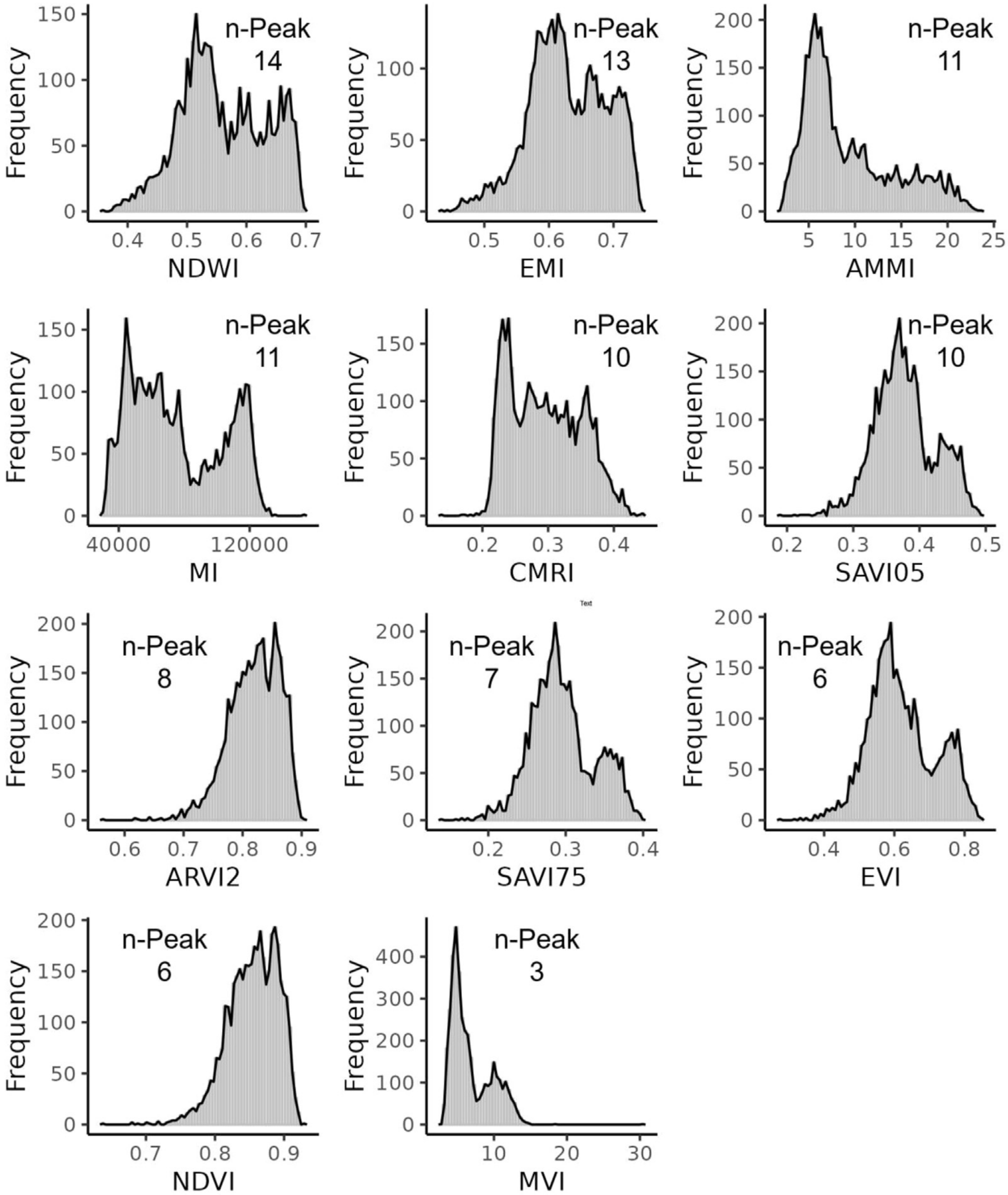

Fig. 3. Histogram of spectral indices.

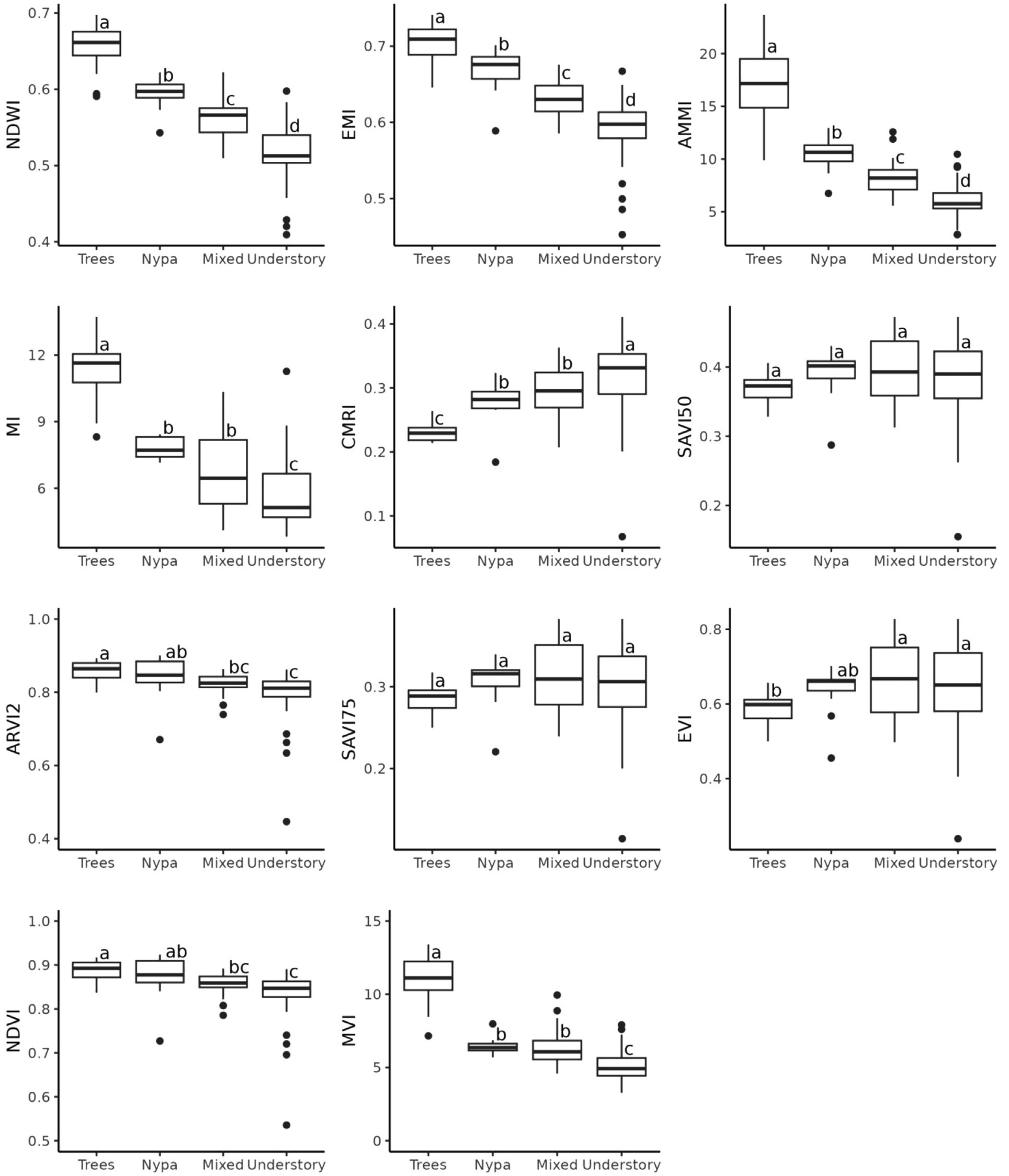

Fig. 4. The box plot displays the spectral indices for the specific type of mangrove vegetation (Mangrove trees, nypa, understorey, and mixed class). The letters are used to represent the significant difference among the categories employing ANOVA and Tukey's test ($p < 0.05$).

Table 3
The threshold values for classes of mangrove vegetation as measured by the chosen spectral indices.

Class	EMI		AMMI		NDWI	
	Min	Max	Min	Max	Min	Max
Mangrove Trees	0.68	≥ 0.68*	10.78	≥ 10.78*	0.62	0.72
Nypa	0.66	0.68	9.63	10.77	0.59	0.62
Mixed	0.61	0.65	6.63	9.63	0.55	0.59
understorey	0.53	0.61	3.12	6.63	0.45	0.55

* Maximum EMI and AMMI values are represented as mangrove trees.

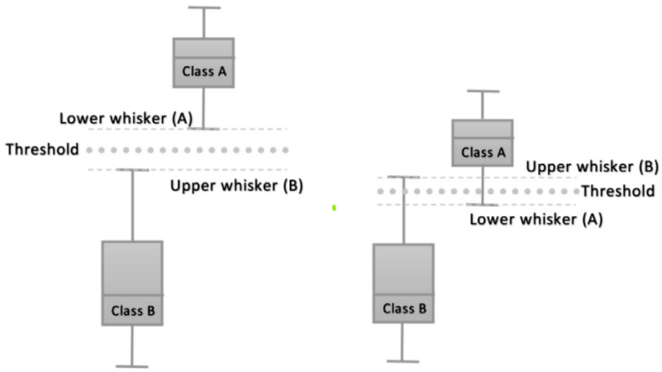

Min Threshold Value (Class A) ≈ Max Threshold Value (Class B) = Threshold Value

= Lower whisker (A) - {0.5*[Lower whisker (A) - Upper whisker (B)]}

= Upper whisker (B) + {0.5*[Lower whisker (A) - Upper whisker (B)]}

The equation is valid only when the spectral index range in Class A follows that of Class B, such as in the case of mangrove trees and nypa in EMI (Fig. 4). For the chosen spectral indices, EMI, AMMI, and NDWI, the threshold values are presented in Table 3. Mangrove trees have the highest EMI and AMMI values, so there is no maximum limit for these two indices. Mangrove trees, on the other hand, do not have the highest NDWI values; instead, the highest values are found in water bodies. Interestingly, terrestrial vegetation is classified as having EMI values lower than the minimum understorey threshold (the value is not shown here).

Evaluation

Fig. 5 displays the outcomes of unsupervised classification utilizing the novel spectral index, EMI, in comparison to AMMI, NDWI, and RF. This study demonstrated that the EMI outperformed other spectral indices and supervised models, with overall accuracy and the Kappa coefficient reached 0.87 and 0.84, respectively (Table 3). Almost all classes have a similar confident producer accuracy of 0.93, but nypa has 0.67. This means that 93 % of the predicted pixels for trees, mixed, and understorey were fitted to the actual pixels. In comparison, only 67 % of nypa was fitted with actual pixels. The user accuracy reveals a different situation, as all classes have relatively high confidence values ranging from 0.78 to 1. It indicates that the actual pixels (referenced data) were relatively fitted to the predicted pixels.

The AMMI model achieved the next highest accuracy, with overall accuracy and the Kappa coefficients of 0.82 and 0.77. However, nypa and mixed classes had low values for both producer and user accuracy. Only mangrove trees and understorey classes appear to be confident in their accuracy. Even mangrove trees class has the same accuracy values as EMI: 0.93 and 0.88 for producer and user accuracy, respectively.

Nypa and mixed classes have significantly lower accuracy than other classes in both producer and user accuracy in several models, including EMI, AMMI, RF, CART, and MD. Mangrove trees and understorey classes, on the other hand, were relatively more confident in all models because their values were higher than nypa and mixed class. It is a good indication, as all models have the potential to distinguish between mangrove tree and understorey communities within mangrove forests using satellite remote sensing. Therefore, there was still a gap in identifying the nypa class.

Moreover, the accuracy assessment results indicate that spectral indices exhibit greater accuracy compared to supervised classification models. RF and SVM are classification models that exhibit satisfactory overall accuracy, whereas CART demonstrates the lowest accuracy, with an overall accuracy of 0.66 and a Kappa coefficient of 0.57 (Table 4).

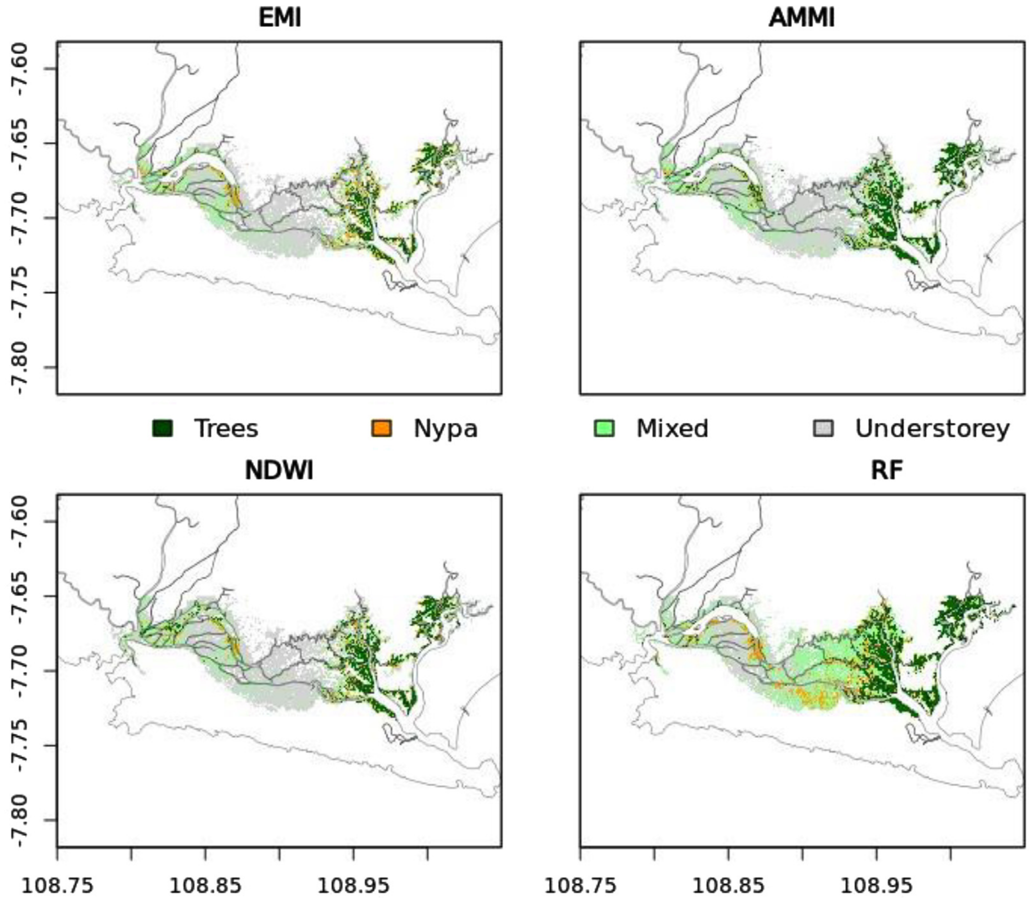

Fig. 5. A comparison mangrove map of Segara Anakan produced by employing the EMI, a novel spectral index in conjuction with two other indices (NDWI and AMMI), as well as the supervised classification model (RF).

Table 4
The accuracy assessment of mapping models.

Class	EMI		NDWI		AMMI		RF		CART		MD		SVM	
	PA	UA	PA	UA	PA	UA	PA	UA	PA	UA	PA	UA	PA	UA
Mangrove Trees	0.93	0.88	0.93	0.88	0.93	0.88	0.93	0.56	1.00	0.56	0.93	0.93	0.93	0.93
Nypa	0.67	1.00	0.27	0.57	0.67	0.77	0.80	0.86	0.53	0.73	0.67	0.50	0.87	0.46
Mixed	0.93	0.88	0.67	0.56	0.73	0.73	0.20	0.43	0.07	0.14	0.40	0.67	0.00	0.00
understorey	0.93	0.78	0.87	0.68	0.87	0.81	0.80	1.00	0.80	1.00	0.60	0.75	0.87	0.87
Non-Mangrove	0.91	0.91	0.91	0.91	0.91	0.91	1.00	0.83	1.00	0.77	0.90	0.64	1.00	0.91
Overall Accuracy	**0.87**		0.72		**0.82**		**0.73**		0.66		0.69		0.71	
Kappa Coefficient	0.84		0.65		0.77		0.66		0.57		0.61		0.64	

PA: Producer Accuracy.
UA: User Accuracy.

Conclusion

The novel spectral index, EMI, serves two functions: it distinguishes between mangrove and terrestrial vegetation while also categorizing mangrove vegetation cover into three distinct classes: mangrove trees, nypa, and understory. The use of this index is essential for mangrove monitoring, as seen in Segara Anakan, where nypa and understory encroachment has resulted in the rapid displacement of mangrove tree populations. The spectral index can be used in a variety of geographical regions, including Indonesia and other parts of the world's mangrove ecosystem. Nonetheless, further investigation is required to determine its suitability. Confirmation is also required to use additional satellite images with SWIR, NIR, and Green spectra for image classification using EMI. Using EMI, an automated mapping process will be economically efficient computing, regardless of whether it is implemented through GEE or another platform.

Ethics statements

Not applicable.

Declaration of generative AI and AI-assisted technologies in the writing process

During the preparation of this work the authors used the Quillbot premium service in order to improve the readability of the manuscript. After using this tool/service, the authors reviewed and edited the content as needed and take full responsibility for the content of the publication.

Declaration of competing interest

The authors declare that they have no known competing financial interests or personal relationships that could have appeared to influence the work reported in this paper.

CRediT authorship contribution statement

Bayu Prayudha: Conceptualization, Methodology, Software, Writing – original draft. **Yaya I. Ulumuddin:** Conceptualization, Methodology, Writing – review & editing. **Vincentius Siregar:** Writing – review & editing, Supervision. **Suyarso:** Writing – review & editing, Supervision. **Syamsul B. Agus:** Writing – review & editing, Supervision. **Lilik B. Prasetyo:** Writing – review & editing, Supervision. **Suyadi:** Investigation, Resources. **Praditya Avianto:** Investigation, Visualization. **Muhammad R. Ramadhani:** Investigation.

Data availability

Data will be made available on request.

Acknowledgments

This research was supported by the capacity building research of COREMAP - CTI BRIN, degree by research program of BRIN - IPB.

References

[1] R.T. Alberto, S.C. Serrano, G.B. Damian, E.E. Camaso, A.R. Biagtan, N.Z. Panuyas, J.S. Quibuyen, Extraction of inland Nypa fruticans (Nipa Palm) using Support Vector Machine, Fifth Int. Confer. Remote Sens. Geoinform. Environ. (RSCy2017) 10444 (2017) 30–37.
[2] E.R. Ardli, M. Wolff, Quantifying habitat and resource use changes in the Segara Anakan Lagoon (Cilacap, Indonesia) over the Past 25 Years, Asian J. Water, Environ. Pollut. 5 (2008) 59–67.
[3] E.R. Ardli, E. Yani, Mangrove damage evaluation using two pecies of Acanthus as a biomonitoring agent, case study: segara Anakan Cilacap, Indonesia, *IOP Conf. Ser. Earth Environ. Sci.* 550 (2020) 012001.
[4] A.B. Baloloy, A.C. Blanco, R.R.C. Raymund Rhommel, K Nadaoka, Development and application of a new mangrove vegetation index (MVI) for rapid and accurate mangrove mapping, ISPRS J. Photogramm. Remote Sens 166 (June) (2020) 95–117.
[5] N.Y. Cárdenas, K.E. Joyce, S.W. Maier, Monitoring mangrove forests: are we taking full advantage of technology? Int. J. Appl. Earth Obs. Geoinf. 63 (2017) 1–14.
[6] L. Carugati, B. Gatto, E. Rastelli, M. Lo Martire, C. Coral, S. Greco, R. Danovaro, Impact of mangrove forests degradation on biodiversity and ecosystem functioning, Sci. Rep 8 (1) (2018) 13298.
[7] Y. Deng, C. Wu, M. Li, R Chen, RNDSI: a ratio normalized difference soil index for remote sensing of urban/suburban environments, Int. J. Appl. Earth Obs. Geoinf. 39 (2015) 40–48.
[8] N.C. Duke, Mangroves, in: D. Hopley (Ed.), Encyclopedia of Modern Coral Reefs. Encyclopedia of Earth Sciences Series, Springer, Dordrecht, 2011.
[9] FAO, The world's mangroves 1980-2005. *FAO For*, Pap 153 (2007) 89.
[10] N.M. Farda, Multi-temporal land use mapping of coastal wetlands area using machine learning in Google earth engine, IOP Confer. Ser 98 (1) (2017) 012042.
[11] I Faridah-Hanum, A Latiff, KR Hakeem, M Ozturk (Eds.), Mangrove Ecosystems of Asia: status, Challenges and Management Strategies, Springer Science & Business Media, 2014.
[12] B.C. Gao, NDWI A normalized difference water index for remote sensing of vegetation liquid water from space, Remote Sens Environ 58 (3) (1996) 257–266.
[13] A.A. Gitelson, Y.J. Kaufman, M.N Merzlyak, Use of a green channel in remote sensing of global vegetation from EOS- MODIS, Remote Sens Environ 58 (3) (1996) 289–298.
[14] K. Gupta, A. Mukhopadhyay, S. Giri, A. Chanda, S. Datta Majumdar, S. Samanta, D. Mitra, R.N. Samal, A.K. Pattnaik, S Hazra, An index for discrimination of mangroves from non-mangroves using LANDSAT 8 OLI imagery, MethodsX 5 (2018) 1129–1139.
[15] F. Hariati, H. Ajiwibowo, I.K. Hadihardaja, J. Nugroho, Modelling Adaptation To Salinity Intrusion in Segara Anakan, Int. J. GEOMATE. 16 (2019) 9–17.
[16] S. Hinrichs, I. Nordhaus, S.J. Geist, Status, diversity and distribution patterns of mangrove vegetation in the Segara Anakan lagoon, Java, Indonesia, Reg. Environ. Change 9 (2009) 275–289.
[17] P. Holtermann, H. Burchard, T. Jennerjahn, Hydrodynamics of the Segara Anakan lagoon, Reg. Environ. Change 9 (4) (2009) 245–258, doi:10.1007/s10113-008-0075-3.
[18] A.R. Huete, A soil-adjusted vegetation index (SAVI), Remote Sens. Environ 25 (3) (1988) 295–309.
[19] A. Huete, K. Didan, T. Miura, E.P. Rodriguez, X. Gao, L.G Ferreira, Overview of the radiometric and biophysical performance of the MODIS vegetation indices, Remote Sens. Environ 83 (2002) 195–213.

[20] M. Ilman, I.T.C. Wibisono, I.N.N. Suryadiputra, State of the art information on mangrove ecosystems in Indonesia, Wetlands Int.-Indonesia Progr., Bogor 19 (2011).
[21] T.C. Jennerjahn, E. Yuwono, Segara Anakan, Java, Indonesia, a mangrove-fringed coastal lagoon affected by human activities, Reg Environ. Change 9 (2009) 231–233.
[22] J. Jones, P.E.R. Dale, A.L. Chandica, M.J. Breitfuss, Changes in the distribution of the grey mangrove Avicennia marina (Forsk.) using large scale aerial color infrared photographs: are the changes related to habitat modification for mosquito control? Estuar Coast Shelf Sci 61 (1) (2004) 45–54.
[23] Y. Kaufman, D. Tanre, Atmospherically resistant vegetation index, IEEE Transac. Geosci. Remote Sens 30 (2) (1992) 260–271.
[24] C. Kuenzer, A. Bluemel, S. Gebhardt, T.V. Quoc, S. Dech, Remote sensing of mangrove ecosystems: a review, Remote Sens 3 (5) (2011) 878–928.
[25] D.T. Lauer, S.A. Morain, V.V. Salomonson, The Landsat program: its origins, evolution, and impacts, Photogramm. Eng. Remote Sensing 63 (7) (1997) 831–838.
[26] M.C. Lukas, Widening the scope: linking coastal sedimentation with watershed dynamics in Java, Indonesia, Reg. Environ. Change 17 (3) (2017) 901–914.
[27] I. Nordhaus, M. Toben, A. Fauziyah, Impact of deforestation on mangrove tree diversity, biomass and community dynamics in the Segara Anakan lagoon, Java, Indonesia: a ten-year perspective, Estuar. Coast. Shelf Sci. 227 (2019) 106300, doi:10.1016/j.ecss.2019.106300.
[28] T. Piekkoontod, B. Pachana, K. Hrimpeng, K. Charoenjit, Assessments of Nipa forest using Landsat imagery enhanced with unmanned aerial vehicle photography, Appl. Environmen. Res 42 (3) (2020) 49–59.
[29] B. Prayudha, V. Siregar, Y.I. Ulumuddin, Prasetyo LB Suyadi, S.B. Agus, Anggraini K Suyarso, The application of Landsat imageries and mangrove vegetation index for monitoring mangrove community in Segara Anakan Lagoon, Cilacap, Central Java, IOP Conf. Ser. Earth Environ. Sci. 944 (2021) 012039, doi:10.1088/1755-1315/944/1/012039.
[30] B. Prayudha, Y.I. Ulumuddin, V. Siregar, Agus SB Suyarso, L.B. Prasetyo, K. Anggraini, A Salatalohi, Geomorphological and hydrological changes play a critical role in mangrove forest degradation in a rapidly shrinking lagoon in Indonesia, AACL Bioflux 16 (1) (2023) 151–167.
[31] J.W. Rouse, R. Haas, J. Schell, D. Deering, Monitoring vegetation systems in the Great Plains with ERTS, NASA special publication 351 (1974) 309.
[32] P. Saenger, Mangrove structure and classification, Mangrove Ecol. Silvic. Conserv. 2 (2002) 183–205, doi:10.1007/978-94-015-9962-7_6.
[33] Stuhler S.C., Leiterer R., Joerg P., Wulf H., Schaepman M. 2016. Generating a cloud-free, homogeneous Landsat-8 mosaic of Switzerland using Google Earth Engine. 10.13140/RG.2.1.2432.0880.
[34] Avianto P. Suyarso, AMMI automatic mangrove map and index: novelty for efficiently monitoring mangrove changes with the case study in musi delta, South Sumatra, Indonesia, Int. J. For. Res. 2022 (2022) 8103242, doi:10.1155/2022/8103242.
[35] A.D. Syakti, C. Demelas, N.V. Hidayati, G. Rakasiwi, L. Vassalo, N. Kumar, P. Prudent, P. Doumenq, Heavy metal concentrations in natural and human-impacted sediments of Segara Anakan Lagoon, Indonesia, Environ. Monit. Assess 187 (2015) 4079.
[36] T.V. Tran, R. Reef, X. Zhu, A review of spectral indices for mangrove remote sensing, Remote Sens 14 (19) (2022) 4868, doi:10.3390/rs14194868.
[37] D. Wang, B. Wan, P. Qiu, Y. Su, Q. Guo, R. Wang, F. Sun, X. Wu, Evaluating the performance of Sentinel-2, Landsat 8 and Pléiades-1 in mapping mangrove extent and species, Remote Sens 10 (9) (2018) 1468.
[38] G. Winarso, A.D. Purwanto, D.M. Yuwono, New mangrove index as degradation /health indicator using Remote Sensing data: segara Anakan and Alas Purwo case study, in: 12th Biennial Conference of Pan Ocean Remote Sensing Conference, 2014, pp. 309–316.
[39] G. Winarso, M.S. Rosid, M. Kamal, W. Asriningrum, C. Margules, J. Supriatna, Comparison of Mangrove Index (MI) and Normalized Difference Vegetation Index (NDVI) for the detection of degraded mangroves in Alas Purwo Banyuwangi and Segara Anakan Cilacap, Indonesia, Ecol. Eng 197 (2023) 107119.
[40] M.A. Wulder, J.C. White, T.R. Loveland, C.E. Woodcock, A.S. Belward, W.B. Cohen, E.A. Fosnight, J. Shaw, J.G. Masek, D.P. Roy, The global Landsat archive: status, consolidation, and direction, Remote Sens. Environ. 185 (2016) 271–283, doi:10.1016/j.rse.2015.11.032.
[41] J. Xue, B. Su, Significant remote sensing vegetation indices: a review of developments and applications, J. Sens. 2017 (2017) 1353691.
[42] E. Yuwono, T.C. Jennerjahn, I. Nordhaus, E.A. Riyanto, M.H. Sastranegara, R. Pribadi, Ecological status of Segara Anakan, Indonesia: a mangrove-fringed lagoon affected by human activities, Asian J. Water, Environ. Pollut 4 (1) (2007) 61–70.